Elsevier Editorial System(tm) for Catena
Manuscript Draft

Manuscript Number: CATENA2990R2

Title: Calibration of an acoustic pipe sensor through bedload traps in a glacierized basin

Article Type: Research Paper

Keywords: bedload monitoring; glacial regime; acoustic methods; calibration; Alps

Corresponding Author: Dr. Andrea Dell'Agnese,

Corresponding Author's Institution: Faculty of Science and technology - Free University of Bolzano - Bozen

First Author: Andrea Dell'Agnese

Order of Authors: Andrea Dell'Agnese; Luca Mao; Francesco Comiti

Abstract: Quantifying sediment transport in small mountain basins is of great relevance to assess the morphological and ecological dynamics of the entire channel network and to predict flood hazards. In high-elevation, glacierized basins, seasonal variability in sediment transport is dramatic, but despite the relevance of such basins in many regions worldwide, very few investigations have tried to quantify it. Since direct methods to assess bedload transport are time consuming and practically challenging at high flows, indirect surrogate methods, allowing continuous measurements over time, are highly desirable. Yet, these methods require calibration to provide reliable estimations. The present research focused on the calibration of an acoustic pipe sensor in the recently established (spring 2011) monitoring station in the Saldur basin, a high-elevation glacierized watershed in the Eastern Italian Alps. The acoustic pipe signal (which is amplified through 6 channels having different gains) was calibrated against samples collected over 26 sampling periods using "Bunte" bedload traps along a cross-section 12 m upstream of the pipe. Samples were collected from June to August 2011 during daily discharge fluctuations (ranging from 1.40 to 3.63 m3s-1) due to snow- and glacier-melt, featuring very different bedload rates (up to 0.14 kg s-1 m-1). In order to calibrate the pipe sensor signal, the average number of impulses was plotted against the corresponding unit bedload rates for the associated bedload sampling periods. As expected, the signal from the two most sensitive channels of the acoustic sensor resulted dampened even at low discharges, and thus could not be used for calibration and bedload assessment. Instead, power laws (R2 from 0.76 to 0.92) relating the number of impulses per minute to unit bedload rate were obtained using channels having intermediate and low sensitivity, with higher correlations associated with the less sensitive channels.

HIGHLIGHTS

- Direct bedload samplings were taken in an Alpine glacierized stream
- Bedload was measured continuously using an acoustic pipe sensor
- Power-law calibration relationships between bedload rates and impacts were derived
- Bedload is better described by using lower sensitivity channels
- For lower sensitivity channels, activation thresholds were identified

CALIBRATION OF AN ACOUSTIC PIPE SENSOR THROUGH BEDLOAD TRAPS IN A GLACIERIZED BASIN

Dell'Agnese A.[1*], Mao L.[2], Comiti F.[1]

(1) Faculty of Science and Technology, Free University of Bolzano, Piazza Università 5, 39100 Bozen-Bolzano, Italy
(2) Department of Ecosystems and Environment, Pontificia Universidad Católica de Chile, Av. Vicuña Mackenna 4860, Macul, Santiago, Chile

*Corresponding author: e-mail: andrea.dellagnese@natec.unibz.it; phone: +39 0471 017603

ABSTRACT

Quantifying sediment transport in small mountain basins is of great relevance to assess the morphological and ecological dynamics of the entire channel network and to predict flood hazards. In high-elevation, glacierized basins, seasonal variability in sediment transport is dramatic, but despite the relevance of such basins in many regions worldwide, very few investigations have tried to quantify it. Since direct methods to assess bedload transport are time consuming and practically challenging at high flows, indirect surrogate methods, allowing continuous measurements over time, are highly desirable. Yet, these methods require calibration to provide reliable estimations. The present research focused on the calibration of an acoustic pipe sensor in the recently established (spring 2011) monitoring station in the Saldur basin, a high-elevation glacierized watershed in the Eastern Italian Alps. The acoustic pipe signal (which is amplified through 6 channels having different gains) was calibrated against samples collected over 26 sampling periods using "Bunte" bedload traps along a cross-section 12 m upstream of the pipe. Samples were collected from June to August 2011 during daily discharge fluctuations (ranging from 1.40 to 3.63 m^3s^{-1}) due to snow- and glacier-melt, featuring very different bedload rates (up to 0.14 kg s^{-1} m^{-1}). In order to calibrate the pipe sensor signal, the average number of impulses was plotted against the corresponding unit bedload rates for the associated bedload sampling periods. As expected, the signal from the two most sensitive channels of the acoustic sensor resulted dampened even at low discharges, and thus could not be used for calibration and bedload assessment. Instead, power laws (R^2 from 0.76 to 0.92) relating the number of impulses per minute to unit bedload rate were obtained using channels having intermediate and low sensitivity, with higher correlations associated with the less sensitive channels.

Keywords: bedload monitoring; glacial regime; acoustic methods; calibration; Alps

1. INTRODUCTION

Bedload transport in small mountain basins represents a fundamental process for the dynamics and equilibrium of the whole channel network. The determination of bedload rates and volumes transported in mountain rivers has always been a major issue, key for flood hazard assessment and mitigation and now increasingly recognized for aquatic ecosystem analysis (Schwendel *et al.*, 2010). Since the first half of the 20th century, different instruments for bedload measurement have been developed. However, the monitoring of bedload flux in rivers is still highly challenging and subject to relevant technical problems (Gray *et al*. 2007). This is even more so for mountain rivers, especially during high water stages. Starting in the 1970s and 1980s, indirect methods (i.e. not directly "sampling" the transported sediment) were developed to overcome the difficulties inherent in direct bedload sampling.

In mountain rivers, which feature steep slopes, coarse and poorly-sorted sediments along with high flow velocities and turbulence, bedload transport can be measured through different methods, both direct and indirect. Direct methods include retention basins that physically trap all or most of the sediment transported through a section, providing an integral value of transport between consecutive surveys of the basin, i.e. do not provide information on transport rates unless sensors (e.g. pressures cells, distance sensors) are installed to monitor continuously the deposition process, as in the case of the Rio Cordon station (Italy, Mao *et al*. 2010), the Gråelva weir (Norway, Bogen and Møen, 2003), or the Pitzbach weir (Austria, Rickenmann and McArdell, 2008; Turowski and Rickenmann, 2009). Such systems are quite expensive in terms of initial installation and are feasible in relatively small streams only. Other stations for direct continuous records of bedload transport utilize different methods, as in the Erlenbach (Switzerland, Rickenmann *et al.*, 2012), where a basket automatically moving below the crest of a check-dam catches the sediment falling into the retention basin downstream. Slot "Reid-type" traps deployed across a section are used in Japan (Mizuyama *et al.*, 2010 b) and Austria (Habersack *et al.*, 2001), and vortex tube samplers were used for some time in the US and Italy (Hayward, 1980; Tacconi and Billi, 1987). Beside fixed instruments, which feature great advantages in terms of continuous bedload records but present high initial costs and mostly require a careful frequent maintenance, bedload can be sampled through portable devices as the "Helley-Smith" samplers (Emmett, 1980) or by "Bunte" bedload traps (Bunte *et al.*, 2004, 2007), which are more suitable for coarse-bedded mountain rivers (Bunte *et al.*,

2008). These instruments are much cheaper than permanent stations, but their deployment presents relevant difficulties at high flows and – importantly – they cannot provide continuous bedload data. Hence, the need to use indirect methods relying on different types of sensors deployed in or near the riverbed, such as vibration sensors, including piezoelectric sensors and velocimeters (Bogen and Møen, 2003; Richardson *et al.*, 2003; Rickenmann and McArdell, 2007; Rickenmann and Fritschi, 2010) and passive acoustic sensors (Bänziger and Burch, 1990; Jagger & Hardisty, 1991; Taniguchi *et al.*, 1992; Rouse, 1994; Thorne and Hanes, 2002; Downing *et al.*, 2003; Froehlich, 2003; Mizuyama *et al.*, 2003; Krein *et al.* 2004; Barton *et al.*, 2010; Belleudy *et al.*, 2010; Mizuyama *et al,*, 2010a; Mizuyama *et al,*, 2010b). Active acoustic methods are also being effectively deployed (Habersack *et al.*, 2010; Rennie and Church, 2010) but not in mountain streams. Other indirect methods effective in coarse-bedded streams include the assessment of cross-sectional variations coupled to particles velocities (Reimann, 1990), which nowadays can be obtained by tagging clasts with transponders (Lamarre *et al.*, 2005; Schneider *et al.*, 2010; Liébault *et al.*, 2012), whereas in the past it was carried out through naturally magnetic particles (Ergenzinger and Custer, 1983; Hassan and Ergenzinger, 2005).

Acoustic detection of bedload by passive sensors has been studied since the 1950s (e.g., Ivicsics, 1956; Johnson and Muir, 1969; Anderson, 1976; Jonys, 1976; Richards and Milne, 1979), with the specific aim of finding out a non-perturbative technique able to keep the flow regime unaltered near the instrument and acquiring data in a continuous way. Previous research revealed the correspondence of variation ranges between bedload and acoustic pulses (Nakaya, 2008) with sound intensity generally increasing with bedload transport rate, and the frequency of the acoustic signal inversely proportional to the diameter of the moving particles (Froehlich, 2003). Nonetheless, in order to properly use an indirect method, the instrument needs to be calibrated with bedload data obtained via direct methods. At the moment, passive acoustic sensors for bedload monitoring in mountain rivers are widely used in Japan (Mizuyama *et al.*, 2010b), whereas elsewhere – namely in Switzerland and Austria – the use of vibration sensors (i.e. velocimeters, more commonly called geophones) has been adopted (Rickenmann *et al.*, 2012; Habersack *et al.*, 2001).

The objective of this paper is to present an on-field calibration through portable "Bunte" bedload traps of an acoustic pipe sensor (called pipe hydrophone or pipe geophone by its Japanese developers, Mizuyama *et al.*, 2003; Mizuyama *et al.*, 2010b), deployed in a glacierized basin (Saldur River, Italian Alps). To our knowledge, the calibration of indirect bedload sensors by means of portable bedload traps has never been carried out before, as this type of sensors have been calibrated either through slot samplers (Habersack *et al.*, 2001; Mizuyama *et al*, 2010b) or by more sophisticated stations (as in the Erlenbach, Rickenmann and McArdell, 2007). Because the

installation and the maintenance of slot samplers in mountain rivers – especially if snow- or glacier-fed – is neither technically easy nor cheap, the possibility of calibrating a relatively inexpensive acoustic sensor such as the pipe sensor through cheap portable traps (< 500 € each) could represent an effective combination to be deployed in such rivers for a continuous bedload monitoring. The bedload sampling carried out to calibrate the acoustic pipe will be first illustrated, followed by the different calibration curves obtained. Finally, the threshold discharges and the related particle size which induces a response of the acoustic pipe will be analysed.

2. STUDY AREA AND METHODS

2.1 The study basin

The study area is the upper Saldur basin (Eastern Italian Alps), whose elevations range from 2150 m a.s.l. (location of the main monitoring site, called LSG as it hosts the lower stream gauge of the monitored watershed) to 3738 m a.s.l. (Weisskugel/Palla Bianca peak), for a total area of 18.6 km^2 (Figure 1). The main glacier hosted in the basin lies between 2700 and 3700 m a.s.l., with a current extent of 2.8 km^2. Therefore, 15% of the basin area is currently glacierized. The Saldur basin belongs to the Ötztal-Stubai complex and mainly consists of orthogneiss. Several rock-glaciers and large moraines are found in the basin, but their connectivity to the main channel appears to be rather limited. Other sediment sources are represented by talus slopes (mostly located at the higher elevations), shallow landslides (of limited extent) and large alluvial/debris fans reaching the valley bottom from the steep tributaries.

The Saldur catchment is characterized by a relatively dry climate, with an annual average precipitation (at 1570 m a.s.l.) of 530 mm in the period 1925 – 2012 (source: Hydrographic Office, Autonomous Province of Bozen-Bolzano). Precipitation occurs in the study area as snowfall from November to late April, but snow storms can occur also during the summer at higher elevations. The hydrological regime of the Saldur River is typical of high-elevation glacier-fed streams, with minimum and maximum flows in winter and summer, respectively. Large floods are associated with early summer rain-on-snow events or convective late summer storms. At the LSG section, diurnal discharge fluctuations due to glacier-melt in late summer range approximately from 1.5 m^3s^{-1} (late morning) to 4 m^3s^{-1} (late afternoon, Penna *et al.*, 2013).

Single-thread reaches are dominant overall, with slopes about 6%, channel width of about 4-6 m, featuring step-pool and cascade characteristics but with occasional glide-run units and lateral bars. The reach just upstream of the main monitoring station LSG is highly confined by the adjacent

hillslopes and features a 6% slope, 5-6 m width, and a bed morphology transitional from plane-bed to step-pool.

The LSG monitoring station is located immediately above the tree line, in proximity to a bridge. It was installed at the narrowest section along the upper Saldur river, where accessibility through an unpaved road for 4WD vehicles is also granted. Channel banks here are stabilized by very large boulders. At this section, water stage is measured (from May to November) every 10 min by a pressure transducer, and stage-water discharge relationship is derived based on several discharge measurements carried out using the salt dilution method, from low flows up to near-bankfull conditions (Penna et al., 2013). A fixed probe measuring water turbidity, electrical conductivity and temperature is installed there as well. Bottle samples for determining the relationship between suspended sediment concentration and turbidity are taken periodically.

2.2 Bedload monitoring

2.2.1 Acoustic pipe sensor

In May 2011, the department of Hydraulic Engineering of the Autonomous Province of Bozen-Bolzano placed a wooden log transversally in the Saldur channel bed at LSG (Figure 2) – where channel width is 3 m – anchored against the boulders of the banks and stabilized by a sort of boulder ramp. A 0.5 m long acoustic pipe, manufactured by Hydrotech Company (Japan), the same as deployed in several Japanese streams since the 1990s (Mizuyama *et al.*, 2003, 2010b) was then attached by metal fittings to the central part of the log – which was previously carved to host it – with half diameter exposed as suggested by the manufacturer and commonly done in Japanese installations, where concrete structures are used instead.

The acoustic pipe sensor is a steel, air-filled pipe with a microphone inside which detects the acoustic vibrations induced by hitting particles (Figure 3). Acoustic pressure waves induced by moving particles hitting the pipe generate a signal amplified by a pre-amplifier and then transmitted to a converter. The converter generates a voltage which is processed through a 6-channel band-path filter (with channel 1 and channel 6 corresponding to the highest and lowest sensitivity, respectively). The band-path filters have lower (2.5 V) and upper (5 V) thresholds, hence an impulse is generated when the output of a channel exceeds 2.5 V. Each channel has a gain of 4 relative to the previous, lesser voltage-output channel, e.g. the 6-channel voltage exiting the converter's amplifier for a 10 mV signal is: channel 6 (x1) = 10 mV; channel 5 (x4) = 40 mV; channel 4 (x16) = 160 mV; channel 3 (x64) = 640; channel 2 (x256) = 2.56 V; channel 1 (x1016) = 10.16 V (for more details, see Mizuyama *et al.*, 2010b). The converted signal is then processed by a

8-channel interval timer (Campbell SDM-INT8) attached to a datalogger (Campbell CR1000), sampling the signal at a frequency of 5 Hz. Both the interval timer and the datalogger were installed inside a case on the river bank, where a solar panel (10W) and a battery (12V) supply the required power to the system. Impulses for each channel are recorded by the datalogger at 1 min intervals.

The instrument was fully operational on July 15th, and recorded data until September 27th, 2011, when the datalogger was removed for the winter season. In 2012 and 2013 reliable data could not be collected due to sediment aggradation on the pipe. The sensor is planned to be moved to a different, more stable section in summer 2014.

2.2.2. Bedload sampling

Data for calibrating the pipe signal were collected by direct measurements of bedload transport rates using "Bunte" traps (4mm mesh size, 20 cm x 30 cm opening, Bunte *et al*., 2007). Because particles smaller than approximately 4 mm are not generally able to generate impulses in the pipe sensor (Mizuyama *et al*., 2010a), sediment collected by the bedload traps should be representative of the bedload fraction detected by the pipe.

Bedload traps were installed at 3 positions across a 5 m wide section located 12m upstream of the pipe at LSG (Figures 4 and 5). The choice of sampling bedload upstream of the pipe rather than downstream was due to the impossibility of having a suitable (regular and wadable at high flows) section downstream of the sensor, where the channel bed becomes rougher and steeper. Certainly, it would have been more ideal to sample directly downstream of the pipe (as done for example with Reid-type slot samplers in Japan, see Mizuyama *et al*. 2010b). However, only a minor part of the sediment moving through the cross-section was trapped in the portable traps (see below) and thus did not reach the pipe during the sampling period. Although such a calibration should be viewed as more "relaxed" and less accurate than that carried out using pit traps, we believe it could be still reasonably accurate for similar complex river settings, where alternative solutions are definitely more expensive.

During July and August 2011, bedload sampling (durations from 5 to 63 min) was carried out during 13 days at different times (from 8 am to 7 pm) in order to capture the daily discharge fluctuations due to snow- and glacier-melt flows (water discharge from 1.40 to 3.63 m^3s^{-1}, Figure 6). Bankfull stage in the LSG reach corresponds to approximately 4 m^3s^{-1}. Preliminary tests showed that unit bedload rates didn't change significantly with variations in the sampling duration.

A total of 95 samples were taken at the 3 different positions across the section (Figure 5, Table 1). The paucity of bedload measurements at position C and the absence of samples taken between B and C was due to the relatively deep and fast flows that made unfeasible to deploy

correctly the bedload traps there. Additionally, due to flow conditions requiring two operators to work at the same sampler during the higher flows, it was not possible to always sample two positions at the same time, as it would be ideal. The bedload samples (a total of 927 kg over the entire season) were then taken to the laboratory, where they were dried, sieved and weighed. The grain size distribution and the bedload transport rate from each sample were then calculated. For each curve, the following characteristics diameters (i.e. quantiles, diameters D_x for which x% of the trapped sediment is finer) were calculated: D_{30} D_{50}, and D_{90}.

The total bedload transport rates for the entire cross-section (Q_s) for each sampling period were then estimated from the samples available. However, because sampling in position C was possible only on one day during the whole season and only for a narrow range of water discharges (1.6 to 2 m^3s^{-1}), it was decided to exclude the few samples taken in C. Hence, a relatively strong assumption was made, i.e. bedload transport in the left half of the cross-section (estimated by samplers A and B) was approximately equal to the right half section. Such hypothesis certainly oversimplifies the variations of bedload transport rates across a section, but it is considered reasonable due to the limited channel width and the relatively straight and symmetrical geometry characterizing the monitored site (Figures 4 and 5). Furthermore, the horizontal wooden log on which the pipe sensor was installed few meters downstream of the sampling sites contributed providing a regular shape and limited vertical changes to the cross-section. In order to calculate the bedload transport rates in the left half of the section, the channel bed portions (i.e. widths) relative to samplers A and B were assessed based on their hydraulic characteristics, such as bed roughness and water depth, and used as weights in averaging the respective transport rates – per unit width – during each sampling period. The transport rate for the entire section was then calculated as twice the transport of the left half. Finally, in those cases when only one sample (A or B) was collected at a specific sampling time, the transport rate per unit width derived from the available sample was considered uniform over the section, and thus simply multiplied by the channel width.

For calibrating the acoustic pipe sensor, a second assumption was made. It has been considered that for each sampling period, bedload transport rates measured (or better estimated) through the "Bunte" traps were representative of the transport rates actually taking place at the pipe section, 12 m downstream. This assumption is justified because i) the bed width "trapped" by the samplers is small compared to entire cross-section (0.6 m vs 5 m, i.e. 12%) and ii) relevant morphological changes (i.e. sediment entrainment or deposition) between the "Bunte" and the pipe sections did not occur, due to the morphological characteristics of the short intervening stream length. This was verified by visual as well as by topographical assessments carried out during the season. Nonetheless, not all the samples were used for calibration because in some cases sediment

aggradation was observed on the pipe sensor itself – despite its cross-section was the narrowest along the channel – making the sensor signal not reliable. Eventually, samples from 26 sampling periods were used for the calibration.

For all the sampled periods, cross-section-averaged unit bedload rates q_s (in kg m^{-1} s^{-1}), later used for pipe calibration, were calculated by dividing Q_s by channel bed width, which remained constant for the measured flow range. The impulses generated by the acoustic pipe were summed (separately for the 6 channels, see section 2.2.1) for each sampling period, and then expressed as number of impulses per minute. Water discharge data (see section 2.1) were averaged over each sampling period.

3. RESULTS

3.1 Variations of bedload transport rates and size with discharge

The relationship between cross-section-averaged unit bedload transport rate q_s (calculated as explained above) and water discharge Q for all the sampling periods is shown in Figure 7. The best fit proved to be in the form of a power law (R^2=0.61) but it is not statistically significant ($p>0.10$) due to the scatter larger than two orders of magnitude for the lowest discharges. Such scatter is partly associated to the seasonal (July vs August) differences in the Q-q_s relationship. Indeed, data gathered during July plot well lower than August for low to intermediate discharges (from 1.40 to 2.80 m^3s^{-1}). Figure 7 shows that very low unit bedload rates (i.e. 0.0001 kg m^{-1} s^{-1}) were observed for the lowest flows sampled (Q=1.4 m^3s^{-1}) corresponding to summer low flows.

Figure 8 shows instead unit bedload transport rates derived directly from the sampling sites (A, B and C, see Figure 5) and their relation with water discharge Q. Best fit curves resulted to be power laws (R^2 equal to 0.67 and 0.46 for A and B, respectively, in both cases statistically significant as $p<0.05$). It can be observed that transport rates measured at site B were on average higher than in A for lower flows, but at medium to high flows the trends converge. Data from site C show low bedload rates, but they are too few – four samples collected in the same day and over a very narrow range of discharge – to build a meaningful relationship with discharge and to make a statistical comparison with sites A and B.

The variation of transported grain size with increasing water discharge is illustrated in Figure 9, where three characteristics diameters (D_{30}, D_{50}, D_{90}) of the sampled sediments are shown. The D_{30} ranges mostly from 5 to 10 mm and the D_{50} from 8 to 16 mm, in both cases with little increase for higher discharges (in both cases statistically significant as $p<0.05$). As to the D_{90}, it

mostly ranges from 10 to 40 mm, with a maximum value of 58 mm for the highest flows sampled, and with a more marked increase associated to higher flows. For all diameters, the exponents of the power regression curves plotted in Figure 9 turn out statistically significant ($p<0.05$). The coarsest sampled clasts were 180 mm (site B, Q=2.2 m^3s^{-1}).

3.2 Relationships between impulses, bedload rates and transported grain size

The relationship between the number of impulses (per minute) registered by the pipe sensor during the sample periods and the associated average water discharge is shown in Figure 10. The most sensitive channels (1 and 2, see section 2.2.1) present for the entire range of discharge a rather constant high number of impulses, regardless of discharge. Channel 3 results always active as well (i.e. throughout the season the number of impulses per minute recorded on this channel was always greater than one) but, unlike channel 1 and 2, a change in the trend is apparent, with a flatter curve for Q about >2 m^3s^{-1}. However, some points plot well below (up to 3 orders of magnitude) the general trend. Channel 4 results always active as well, with data ranging over three orders of magnitude and a minimum value of 1 impulse per minute reached at discharges around 1.3 m^3s^{-1}. The overall trend of impulses with discharge for channel 4, as well as that for channel 5, appears to be more well defined when compared to the more sensitive channels. Nonetheless, for both channels 4 and 5, a constant number of impulses per minute is apparent for discharges approximately > 3.5 m^3s^{-1}. Yet, data for such high discharge values are very limited. For channel 6, a meaningful trend is less obvious, and similarly to channels 4 and 5, for the higher discharges the impulse rates remain constant, although much smaller than those of the more sensitive channels.

Hence, for channels 4, 5 and 6 it was possible to identify the lowest discharge associated to bedload impulses detected by the acoustic pipe. Discharge activation thresholds were defined as those corresponding to the lowest non-null number (≥ 1) of impulses per minute recorded by each of the channels. Applying this method, the thresholds were determined to be 1.2 m^3s^{-1} for channel 4, 1.3 m^3s^{-1} for channel 5, and 1.4 m^3s^{-1} for channel 6. To obtain a better understanding of these thresholds, the relationship between transported particle size and the response of each pipe channel was then investigated (Figure 11). The graph shows clearly that the most sensitive channel (channel 1) are not suitable for deriving a threshold in terms of grain size, paralleling the relationship between impulses and water discharge (Figure 10). A similar pattern is shown by channel 2 as well (graph not shown). On the other hand, the least sensitive channel (channel 6) presents a clear increasing trend between grain size and number of impulses, with D_{50}=6.6 mm and D_{90}=14.1 mm associated to impulse rates close to 1, i.e. at the threshold as defined above. A similar trend is also

306 presented by Channel 3 when considering the D_{90} plot (threshold diameter 7.5 mm), while it
307 remains uncertain when considering the D_{50} plot (Figure 11). Threshold diameters for channels 4-5
308 are between 5.5 and 6 mm, and between 7.5 and 9 mm, respectively, considering D_{50} and D_{90}
309 (graphs not shown).
310 In order to calibrate the pipe sensor signal, the average number of impulses per minute
311 during a bedload sampling period was plotted against the corresponding cross-section-averaged unit
312 bedload rates. For each channel of the sensor, we tested two different equation types to link the two
313 variables: a linear relationship, $q_s = AN + B$, and a power law, $q_s = \alpha N^{\beta}$, where N is the average
314 number of impulses per minute recorded by the sensor and A, B, α and β are the coefficients and the
315 exponent determined by statistical regression. The results of the regression analysis, for both
316 models, are presented in Tab. 3.
317 The power law model performs better for channels 2 to 6 (see R^2 values in Table 2) whereas
318 the linear model presents a slightly higher R^2 only for channel 1, but for this channel the parameters
319 are not statistically significant. As showed in Figure 12 and Table 2, the lower the sensitivity of the
320 pipe channel, the better the goodness of fit. Channels 1 and 2 clearly appear to be not adequate for
321 assessing bedload in such bedload active stream, with signal saturation (as visible also in Figure 10)
322 present also at very low bedload rates.
323
324 **4. DISCUSSION**
325
326 The calibration of acoustic pipe sensors had been previously carried out in Japan both in the
327 field and in the lab by the same developers of the instrument (Mizuyama *et al.*, 2010a, 2010b). In
328 the flume tests they conducted, it was observed that the pipe thickness limits the sensitivity of the
329 instrument to grain size of 8 mm. Smaller particles (4 mm) could be detected by the less sensitive
330 channels, while higher sensitivity channels are not able to record pulses because of the vibrations of
331 the metallic tube induced by the high bedload discharge (see Mizuyama *et al.*, 2010a). A threshold
332 size of 4 mm was also indicated by Mizuyama *et al* . (2010b) based on field evidence. Results on
333 the activation thresholds found in the Saldur River show similar outcomes, inasmuch the D_{50} of the
334 bedload samples collected at the impulse threshold is around 6 mm for all the channels, whereas the
335 D_{90} is about 7.5 mm for channels 1-4 but increases to about 9 mm and 14 mm for channels 5 and 6,
336 respectively (Table 3).
337 Mizuyama *et al.* (2010b) argued that a linear functional relationship is to be expected when
338 linking the number of impulses recorded by the pipe sensor to bedload rates, and the equations they
339 proposed from their field calibration were linear, with R^2 ranging from 0.54 to 0.84 depending on

the intensity of bedload rates. Data collected in the Saldur River indicates instead that for all the pipe channels - except channel 1 for which calibration curves are not statistically meaningful – the power law model gives a better fit, although for some channels the difference with the linear model is minimal. Indeed, further calibration studies carried out by Japanese researchers (Mizuyama, personal communication) seem to confirm that power laws could work best for all the channels. The issue of linear vs non-linear models applies also to geophone data, like in the case of the Erlenbach monitoring station (see Rickenmann and McArdell, 2007), where two different relationships relating the sum of the number of impulses recorded during an event to the sediment volume transported were established. These authors highlighted that even though both equations presented the same goodness of fit (R^2=0.87) and comparable standard errors (S_E=0.443 for the linear regression, and S_E=0.457 for the power law), the linear relationship was to be preferred, because the 'best' coefficient in the power law was related to the magnitude of the values used for the calibration, i.e., the coefficient would have changed depending on integration and calibration interval, underestimating the sediment volumes involved in a single event (Rickenmann and McArdell, 2007). Standard errors were calculated for the different calibration laws obtained in the Saldur River (Table 2). The standard errors for channels 1 and 5 associated to power laws are slightly lower than for the linear equations, whereas for the other channels linear regressions feature slightly lower standard errors, with the maximum difference for channel 4 (0.032 and 0.019 for power and linear models, respectively).

In the Saldur River, the higher sensitivity channels 1 and 2 turned out to be saturated even at the lowest flow discharge sampled, which were characterised by a bedload flux of about $2*10^{-5}$ kg $s^{-1}m^{-1}$, mostly composed of medium-sized gravel. Channel 3 presents an apparent saturation for Q > 3 m^3s^{-1}, which is a flow rate easily exceeded during daily snow- and glacier-melt events. On the other hand, channels 5 and 6 are not able to adequately detect bedload transport at the lower discharges, as they present activation thresholds larger than the other channels. Hence, channel 4 seems to be the most appropriate one to be used alone in order to estimate bedload rates in the Saldur River, based on the combination of goodness of fit (Table 2) and low activation thresholds.

Finally, it is relevant to point out how seasonal variations in bedload transport seem to occur in the Saldur River, as suggested from Figures 7 and 10, where July and August clouds do not overlap, with August featuring on average higher bedload rates and number of impulses recorded at the pipe sensor for similar water discharges, especially for low to intermediate flows. Also, different daily hysteretic cycles in bedload-water flow are observed (Mao *et al.*, 2014), and both phenomena are most likely due to the activation of high-elevation different sediment sources (proglacial area and subglacial channels) during late glacial melt. However, these differences appear to be quite

negligible in the bedload calibration plots (i.e. in the relationships between number of impulses and unit bedload rates, Figure 12) thereby permitting the use of a single calibration equation for the entire hydrological period, from late snowmelt-early glaciermelt (July) to late glacier melt flow (August-September). Indeed, this work is the first addressing the use of acoustic pipe sensors in glacierized basins, and further observations are needed to understand how seasonal changes in bedload composition might affect the sensor signal and its calibration.

5. CONCLUSIONS

The acoustic pipe sensor appears to be a reliable, cheap instrument for continuous bedload monitoring in mountain rivers. In Japan, the instrument was calibrated by relating the registered number of impulses to the bedload rates obtained by a Reid-type slot sampler placed immediately downstream of the pipe (Mizuyama *et al,*, 2010b). Even if Reid-type slot samplers feature several advantages for bedload monitoring (e.g. the possibility to analyse in detail the temporal variation of bedload flux), in the Saldur River the "Bunte" traps have shown to be a valid alternative for the calibration of indirect bedload sensors in rivers where the former samplers cannot be installed Additionally, as Bunte traps are easier to deploy, they would allow the use of acoustic pipes even in very narrow, steep high mountain rivers, actually broadening the field of application of this type of instrument. Hence, by deploying such traps from low to near-bankfull flows, reasonable calibration curves for the sensor were obtained. It was found that the lower the sensitivity of the acoustic pipe channel, the higher the overall correlation with bedload rates. However, channel 6 (i.e. the least sensitive) does not perform well at low discharges (too small particles being transported) while, at higher discharges, the highest sensitivity channels (i.e. 1 and 2) become saturated and the signal from less sensitive channels becomes more relevant. A good compromise for determining bedload rates in similar rivers seems be the analysis of channel 4 or its combined use with 5.

6. ACKNOWLEDGEMENTS

This research was funded by the projects "Effects of climate change on high-altitude ecosystems" (Free University of Bozen-Bolzano), "GESTO" (Aut. Province of Bozen-Bolzano), and "EMERGE: Retreating glaciers and emerging ecosystems in the Southern Alps" (Herzog-Sellenberg- und Ritter-Stiftung im Stifterverband für die Deutsche Wissenschaft). During the research, LM was supported by an Incoming Researcher Fellowship provided by the Autonomous Province of Bozen-Bolzano whilst based at the Free University of Bozen-Bolzano. The Dept. of

Hydraulic Engineering of the Aut. Province of Bolzano supported the installation of the monitoring system, and T. Mizuyama, M. Nonaka, J. Turowski and D. Rickenmann are warmly thanked for suggestions and discussions on data analysis. Four anonymous reviewers are greatly thanked for very helpful comments which ameliorated substantially the manuscript.

7. REFERENCES

Anderson, M.G., 1976. An inexpensive circuit design for the acoustic detection of oscillations in bedload transport in natural streams. Earth Surface Processes, v. 1, pp. 213-217.

Bänziger R., Burch H., 1990. Acoustic sensors as indicators for bed load transport in a mountain torrent. Hydrology in Mountainous Regions I., Lang H, Musy A. (eds), Int'l Assoc. Hydrol. Sci. Publ. 193, pp. 207-214.

Barton, J.S., Slingerland, R.L., Pittman, S., Gabrielson, T.B., 2010. Monitoring coarse bedload transport with passive acoustic instrumentation: A field study. US Geol. Surv. Scientific Investigations Report, 5091.

Belleudy, P., Valette, A., Graff, B., 2010. Passive Hydrophone Monitoring of Bedload in River Beds: First Trials of Signal Spectral Analysis. Gray, JR, Laronne, JB, and Marr, JDG, Bedload-surrogate monitoring technologies, US Geol. Surv. Scientific Investigations Report, 5091.

Bogen J, Møen K., 2003. Bed load measurements with a new passive acoustic sensor. Erosion and Sediment Transport Measurement in Rivers: Technological and Methodological Advances, Bogen J, Fergus T, Walling DE (eds). IAHS Publication 283, International Association of Hydrological Sciences, Wallingford; pp. 181–192

Bunte, K., Abt, S.R., Potyondy, J.P., Ryan, S.E., 2004. Measurement of coarse gravel and cobble transport using a portable bedload trap. Journal of Hydraulic Engineering 130(9), pp 879-893

Bunte, K., Swingle, K.W., Abt, S.R., 2007. Guidelines for using bedload traps in coarse-bedded mountain streams: Construction, installation, operation and sample processing. US Department of Agriculture, Forest Service, Rocky Mountain Research Station.

Bunte, K., Abt, S.R., Potyondy, J.P., & Swingle, K.W., 2008. A comparison of coarse bedload transport measured with bedload traps and Helley-Smith samplers. Geodinamica Acta, 21 (1-2), pp. 53-66.

Downing J, Farley P.J., Bunte K, Swingle K, Ryan S.E., Dixon M., 2003. Acoustic gravel-transport sensor: description and field tests in Little Granite Creek, Wyoming, USA. Erosion and

Sediment Transport Measurement in Rivers: Technological and Methodological Advances, Bogen J, Fergus T, Walling DE (eds). IAHS Publication 283, International Association of Hydrological Sciences, Wallingford, pp. 193-20

Emmett, W.W., 1980. A Field Calibration of the Sediment Trapping Characteristics of the Helley-Smith Bedload Sampler, Geol. Survey Prof. Paper 1139, Washington, DC., 44 pp.

Ergenzinger P, Custer S.G., 1983. Determination of bedload transport using naturally magnetic tracers: first experiences at Squaw Creek, Gallatin County, Montana. Water Resources Research 19, pp. 187–193.

Froehlich W., 2003. Monitoring bed load transport using acoustic and magnetic devices. Erosion and Sediment Transport Measurement in Rivers: Technological and Methodological Advances, Bogen J, Fergus T, Walling DE (eds). IAHS Publication 283, International Association of Hydrological Sciences, Wallingford, pp. 201–210.

Gray J.R., Laronne J.B., Marr, J.D.G., 2007. Measuring bed load discharge in rivers. Bedload - Surrogate Monitoring Workshop Minneapolis, Minnesota, 11–14 April 2007. Eos, Transactions American Geophysical Union, 88 (45), pp. 471-471.

Habersack H.M., Nachtnebel H.P., Laronne J.B., 2001. The continuous measurement of bedload discharge in a large alpine gravel bed river. Journal of Hydraulic Research 39, pp. 125–133.

Habersack, H., Seitz, H., Liedermann, M., 2010. Integrated automatic bedload transport monitoring. Bedload-surrogate monitoring technologies, SIR, 5091, pp. 218-235.

Hassan, M.A., Ergenzinger, P., 2005. Use of Tracers in Fluvial Geomorphology. Tools in Fluvial Geomorphology, edited by D. H. P. Dr G. Mathias Kondolf, pp. 397-423.

Hayward, J.A., 1980. Hydrology and stream sediments in a mountain catchment. Special Publication 17 (PhD dissertation, Lincoln College, Canterbury), Tussock Grasslands and Mountain Lands Institute, New Zealand, 235 pp.

Ivicsics, L., 1956. Acoustic observation of bedload transportation. Különlenyomat a Hidroloiai Közlöny v. 4, pp. 242-247.

Jagger, K.A. and Hardisty, J., 1991. Higher frequency acoustic measurements of coarse bedload transport. Proc. Coastal Sediments '91, American Soc. Civil Engineers. N.Y. pp. 2187-2198.

Johnson, P., Muir, T.C., 1969. Acoustic detection of sediment movement. Jour. Hydraul. Research, v. 7, pp. 519-540.

Jonys, C.K., 1976. Acoustic measurements of sediment transport. Department of Fisheries and the Environment, Canada, 66, 114 pp.

Krein A., Symader W., Eiden M., Klinck H., Bierl R., 2004. Entwicklung und Einsatz eines hydroakustischen Messsystems zur Untersuchung der Dynamik des Geschiebetransportes

476 und quantitativen sowie qualitativen Charakterisierung des bewegten Materials. Hydrologie
477 und Wasserbewirtschaftung 48(5), pp. 172–181.
478 Lamarre, H., MacVicar, B., Roy, A.G., 2005. Using Passive Integrated Transponder (PIT) Tags to
479 Investigate Sediment Transport in Gravel-Bed Rivers. Journal of Sedimentary Research,
480 75(4), pp. 736-741.
481 Liébault, F., Bellot, H., Chapuis, M., Klotz, S., Deschâtres, M., 2012. Bedload tracing in a high‐
482 sediment‐load mountain stream. Earth Surface Processes and Landforms, 37(4), 385-399.
483 Mao, L., Comiti, F., Lenzi, M.A., 2010. Bedload Dynamics in Steep Mountain Rivers: Insights
484 from the Rio Cordon Experimental Station (Italian Alps). Published online as part of U.S.
485 Geological Survey Scientific Investigations Report 2010-5091, pp 253-265.
486 Mao, L., Dell'Agnese, A., Huincache, C., Penna, D., Engel, M., Niedrist, G., Comiti, F. (2014).
487 Bedload hysteresis in a glacier-fed mountain river. Earth Surf. Process. Landforms. doi:
488 10.1002/esp.3563
489 Mizuyama T., Fujita M., Nonaka M., 2003. Measurement of bed load with the use of hydrophones
490 in mountain torrents. Erosion and Sediment Transport Measurement in Rivers:
491 Technological and Methodological Advances, Bogen J, Fergus T, Walling DE (eds). IAHS
492 Publication 283, International Association of Hydrological Sciences, Wallingford, pp. 222–
493 227.
494 Mizuyama, T., Oda, A., Laronne, J.B., Nonaka, M., Matsuoka, M., 2010a. Laboratory Tests of a
495 Japanese Pipe Geophone for Continuous Acoustic Monitoring of Coarse Bedload. Published
496 online as part of U.S. Geological Survey Scientific Investigations Report 2010-5091, pp
497 319-335.
498 Mizuyama, T., Laronne, J.B., Nonaka, M., Sawada, T., Satofuka, Y., Matsuoka, M., Yamashita, S.,
499 Sako, Y., Tamaki, S., Watari, M., Yamaguchi, S., Tsuruta, K., 2010b. Calibration of a
500 passive acoustic bedload monitoring system in Japanese mountain rivers. Published online
501 as part of U.S. Geological Survey Scientific Investigations Report 2010-5091, pp 296-318.
502 Nakaya, H., 2008. A case study of influences on the bed load detection rate of hydrophone system
503 exerted by flow discharges, JSECE, Vol.61, No.4, pp.12–20
504 Parker, G., Dhamotharan, S., & Stefan, H. (1982). Model experiments on mobile, paved gravel bed
505 streams. *Water Resources Research*, *18*(5), 1395-1408.
506 Penna, D., Mao, L., Comiti, F., Engel, M., Dell'Agnese, A., Bertoldi G., 2013. Hydrological effects
507 of glaciermelt and snowmelt in a high-elevation catchment. Die Bodenkultur: Band 64, Heft
508 3-4.

509 Reimann R., 1990. Korrelative Durchsatzmessung von Geschiebe in offenen Gerinnen.
510 Oesterreichische Wasserwirtschaft 42, pp. 43–46.
511 Rennie, C. D., Church, M., 2010. Mapping spatial distributions and uncertainty of water and
512 sediment flux in a large gravel bed river reach using an acoustic Doppler current profiler.
513 Journal of Geophysical Research, Earth Surface (2003–2012), 115(F3).
514 Richards, K.S., Milne, L.M., 1979. Problems in the calibration of an acoustic device for the
515 observation of bedload transport, Earth Surface Processes and Landforms, v. 4, pp. 335-346.
516 Richardson K., Benson I., Carling P.A., 2003. An instrument to record sediment movement in
517 bedrock channels. Erosion and Sediment Transport Measurement in Rivers: Technological
518 and Methodological Advances, Bogen J, Fergus T, Walling DE (eds). IAHS Publication 283,
519 International Association of Hydrological Sciences, Wallingford, pp. 228–235.
520 Rickenmann, D., McArdell, B.W., 2007. Continuous measurement of sediment transport in the
521 Erlenbach stream using piezoelectric bedload impact sensors. Earth Surface Processes and
522 Landforms, 32, pp. 1362–1378.
523 Rickenmann, D., McArdell, B.W., 2008. Calibration of piezoelectric bedload impact sensors in the
524 Pitzbach mountain stream. Geodinamica Acta, 21/1-2, pp. 35-52.
525 Rickenmann, D., Fritschi, B., 2010. Bedload transport measurements using piezoelectric impact
526 sensors and geophones. Proceedings of International Bedload-Surrogate Monitoring
527 Workshop.
528 Rickenmann, D., Turowski, J.M., Fritschi, B., Klaiber, A., Ludwig, A., 2012. Bedload transport
529 measurements at the Erlenbach stream with geophones and automated basket samplers.
530 Earth Surface Processes and Landforms, 37(9), pp. 1000-1011.
531 Rouse, H.L., 1994. Measurement of bedload gravel transport: the calibration of a self-generated
532 noise system. Earth Surface Processes and Landforms (Tech. & Software Bulletin), v. 19, pp.
533 789-800.
534 Schneider, J., Hegglin, R., Meier, S., Turowski, J.M., Nitsche, M., Rickenmann, D., 2010. Studying
535 sediment transport in mountain rivers by mobile and stationary RFID antennas. River Flow,
536 Vol. 2010, pp. 1723-1730.
537 Schwendel, A.C., Death, R.G., & Fuller, I.C., 2010. The assessment of shear stress and bed stability
538 in stream ecology. Freshwater Biology, 55(2), pp. 261-281.
539 Tacconi, P., Billi, P., 1987. Bed load transport measurement by a vortex-tube trap on Virginio
540 Creek, Italy. Sediment Transport in Gravel-Bed Rivers. C.R. Thorne, J.C. Bathurst, and R.D.
541 Hey (eds.), John Wiley, Chichester, pp. 583-615.

Taniguchi S., Itakura Y., Miyamoto K., Kurihara J., 1992. A new acoustic sensor for sediment discharge measurement. Erosion and Sediment Transport Monitoring Programes in River Basins, Bogen J, Walling DE, Day TJ (eds). IAHS Publication 210, International Association of Hydrological Sciences, Wallingford, pp. 135–142.

Thorne P.D., Hanes D.M., 2002. A review of acoustic measurements of small-scale sediment processes. Continental Shelf Research 22, pp. 603–632.

Turowski, J.M, Rickenmann, D., 2009. Tools and cover effects in bedload transport observations in the Pitzbach, Austria. Earth Surface Processes and Landforms, 34(1), pp. 26-37.

FIGURES

Figure 1 - Map and location of the Saldur basin, showing the position of the monitoring station (LSG). The Matsch glacier is visibile in the northern part of the catchment.

Figure 2 – Photo showing the works by the Dept. of Hydraulic Engineering of the Autonomous Province of Bolzano for the installation of the acoustic pipe in the Saldur River (section LSG, May 2011). Stream water was diverted to place a wooden log on the channel bottom, later stabilized by large rocks forming a ramp. The acoustic pipe was then fixed to the log by metal braces. A semi-circular slot – visible in the image – had been previously carved to host approximately half the diameter of the pipe.

Figure 3 – The 0.5m long acoustic pipe sensor manufactured by Hydrotech Company (Japan) installed on the wooden log in the the Saldur River (LSG site).

Figure 4 - Bedload sampling by portable "Bunte" traps immediately upstream of the LSG section during high glacier-melt flows. Three sampling sites were monitored simultaneously, and operators had to keep the trap in the correct position (i.e. flush with the metal plate underneath) for the entire sampling time due to the extremely turbulent conditions.

Figure 5 – Positions of bedload traps along the channel cross-section in the Saldur River. The central part of the section was not sampled due to unfavourable conditions (i.e. irregular coarse bed and too high flow velocities).

Figure 6 – Direct sampling periods during Summer 2011. Orange and green lines represent the beginning and the end of each sampling period, respectively. Samples were taken over five periods during 2011: 12^{th} – 17^{th} July, 21^{st} July, 2^{nd} – 3^{rd} August, 9^{th} – 10^{th} August, 24^{th} – 25^{th} August.

Figure 7 – Semi-log plot of water discharge (Q) versus cross-section-averaged unit bedload rates (q_s) for the entire 2011 season. The overall trend is presented, as well as the seasonal differences between July and August samples. Based on power functions, R^2 results to be 0.63 for both periods, and 0.61 analyzing them together.

Figure 8 – Semi-log plot of water discharge (Q) versus unit bedload rates (q_s) measured at each of the sampling sites (A, B and C, see Figure 5).

Figure 9 –.Characteristic diameters (D_{30}, D_{50}, D_{90}) of the transported sediment collected by the "Bunte" traps plotted versus the associated water discharge at the time of bedload sampling.

Figure 10 – Semi-log plots showing the number of impulses per minute detected by the acoustic pipe for the different sensitivity channels (1 to 6) as a function of the corresponding water discharge (see Table 3).

Figure 11 – Relationship between the number of impulses per minute detected by three of the acoustic sensor's channels (1, 3 and 6, from above to below respectively) and two characteristics diameters (left D_{50}, right D_{90}) of the transported sediment sampled during the same period.

Figure 12 – Calibration relationships (cross-section-averaged unit bedload rates q_s vs number of impulses) for the different sensitivity channels of the acoustic pipe sensors, expressed as power laws (see Table 3).

TABLES

Table 1 – Summary of the bedload sampling activity in the Saldur River site during Summer 2011 (t sampling duration, N number of samples, Q water discharge, h flow depth, w sampled sediment weight, q_s unit bedload rate).

Table 2 – Summary of the coefficients, exponents, R^2, standard errors and p-values for the different equations (both power and linear)relating unit bedload rate to the number of impulses of the acoustic pipe's different amplification channels (see Figure 12).

Table 3 – Characteristics diameters of the bedload samples associated to the minimum number of impulses recorded by each of sixchannels of the acoustic pipe sensor (see Fig. 10). Only for channels 4-6 (the three less sensitive) these grain sizes can be actually interpreted as their activation thresholds, as channels 1-3 always recorded impulses.

Figure 1

Click here to download high resolution image

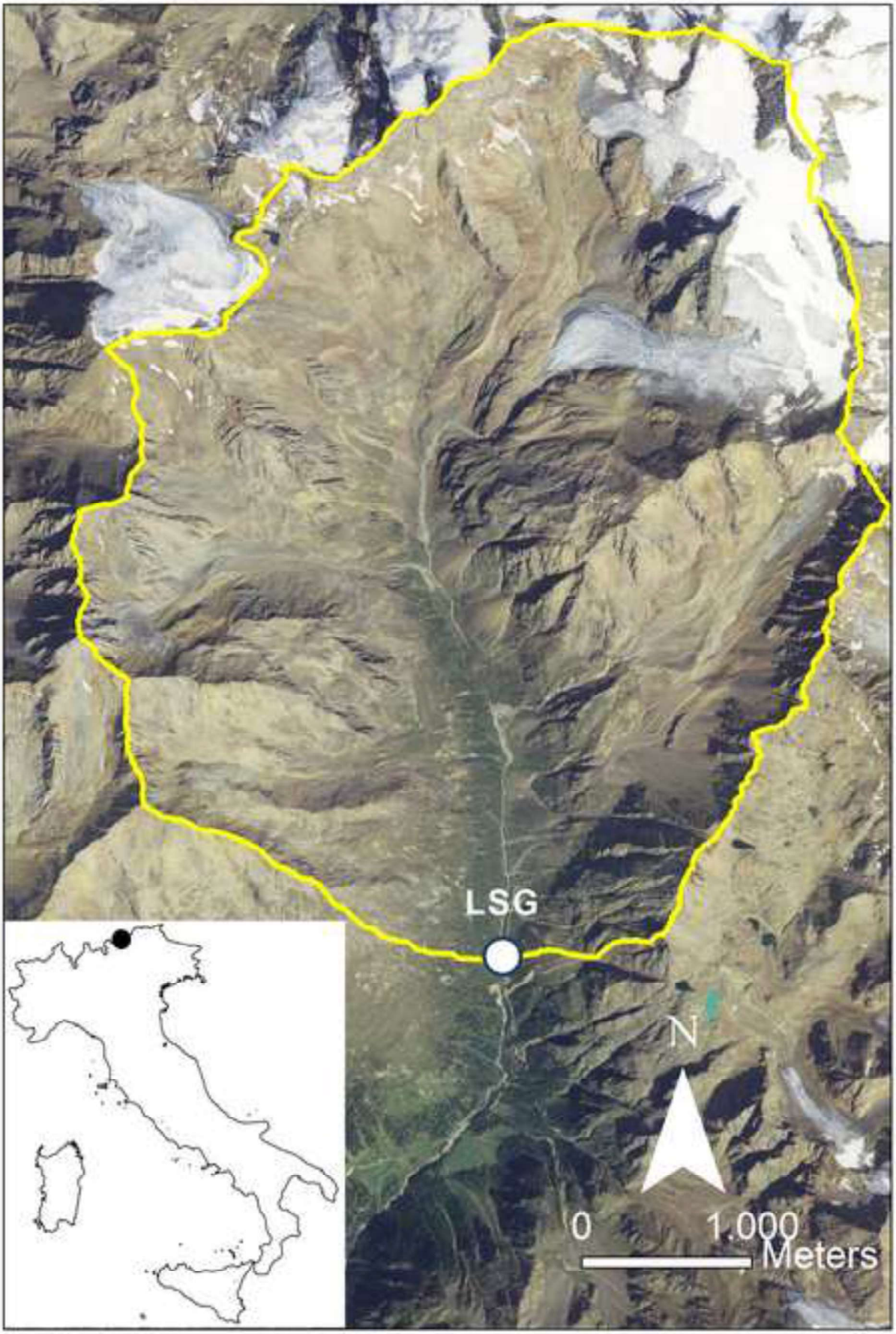

Figure 2

Click here to download high resolution image

Figure 3

Click here to download high resolution image

Figure 4

Click here to download high resolution image

Figure 5
Click here to download high resolution image

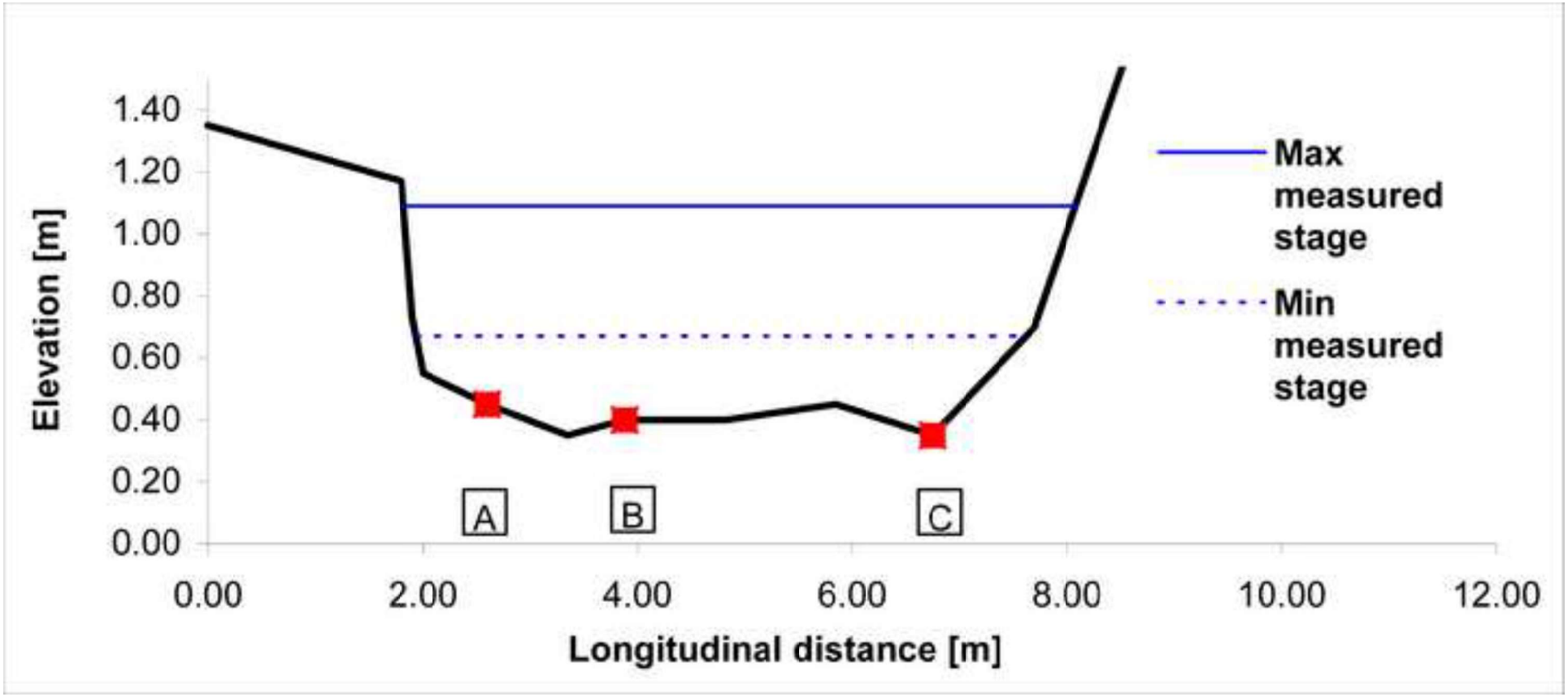

Figure 6

Click here to download high resolution image

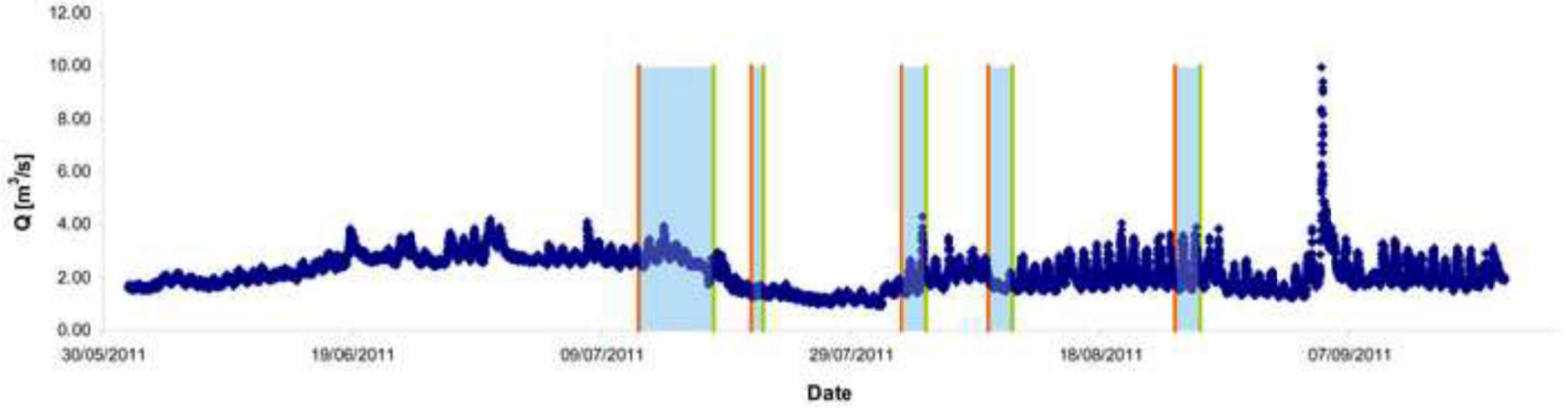

Figure 7

Click here to download high resolution image

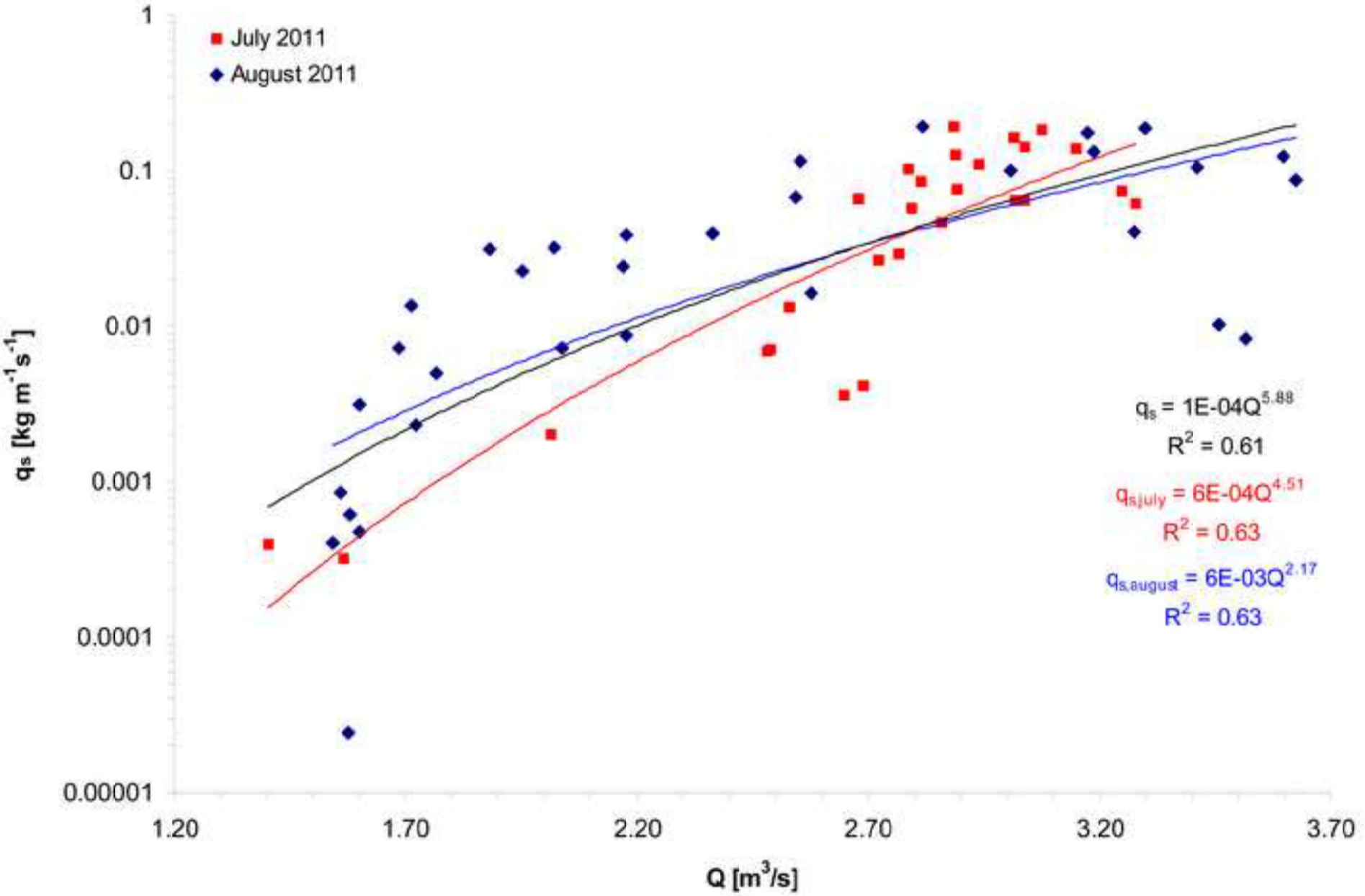

Figure 8

Click here to download high resolution image

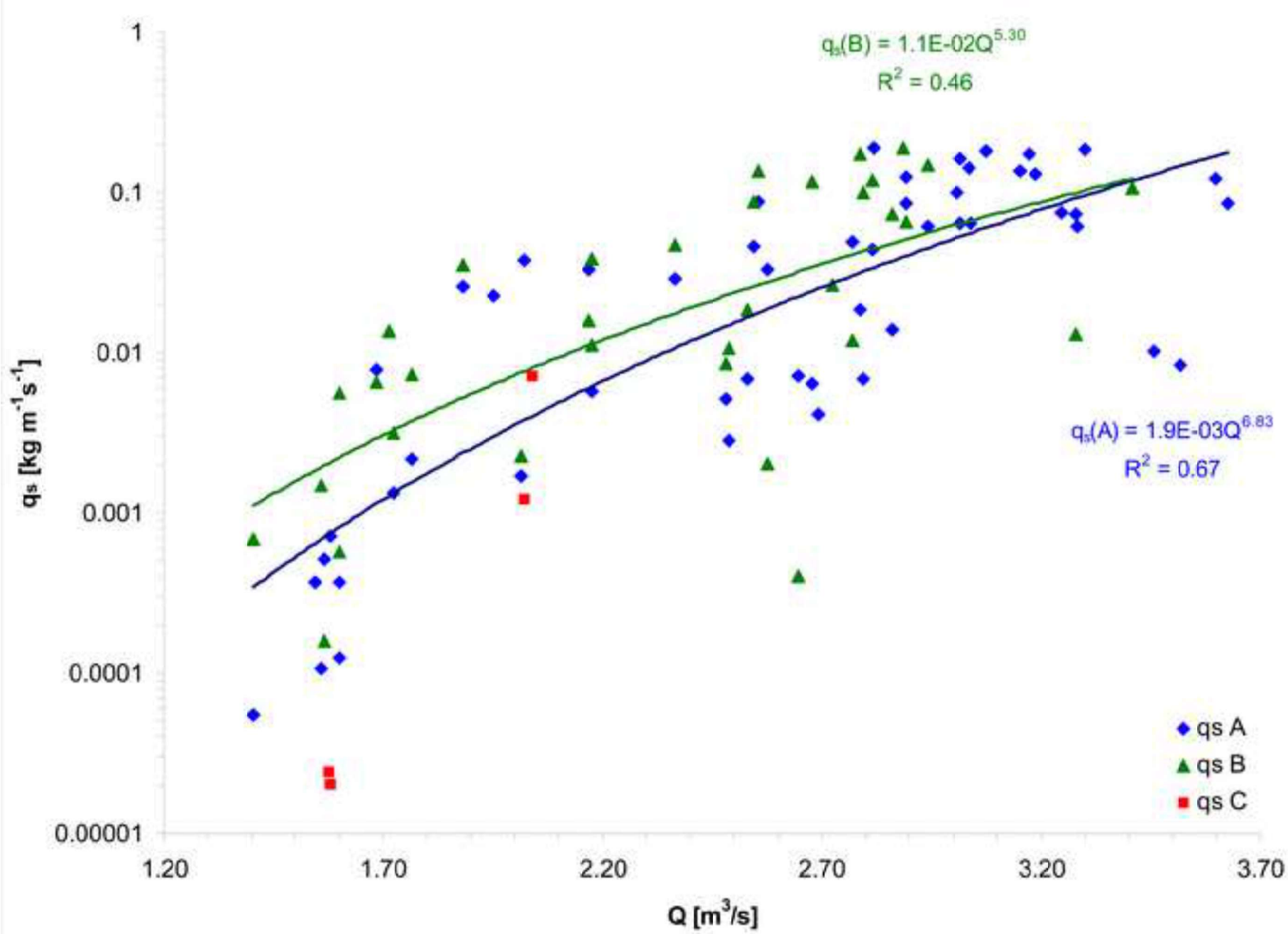

Figure 9

Click here to download high resolution image

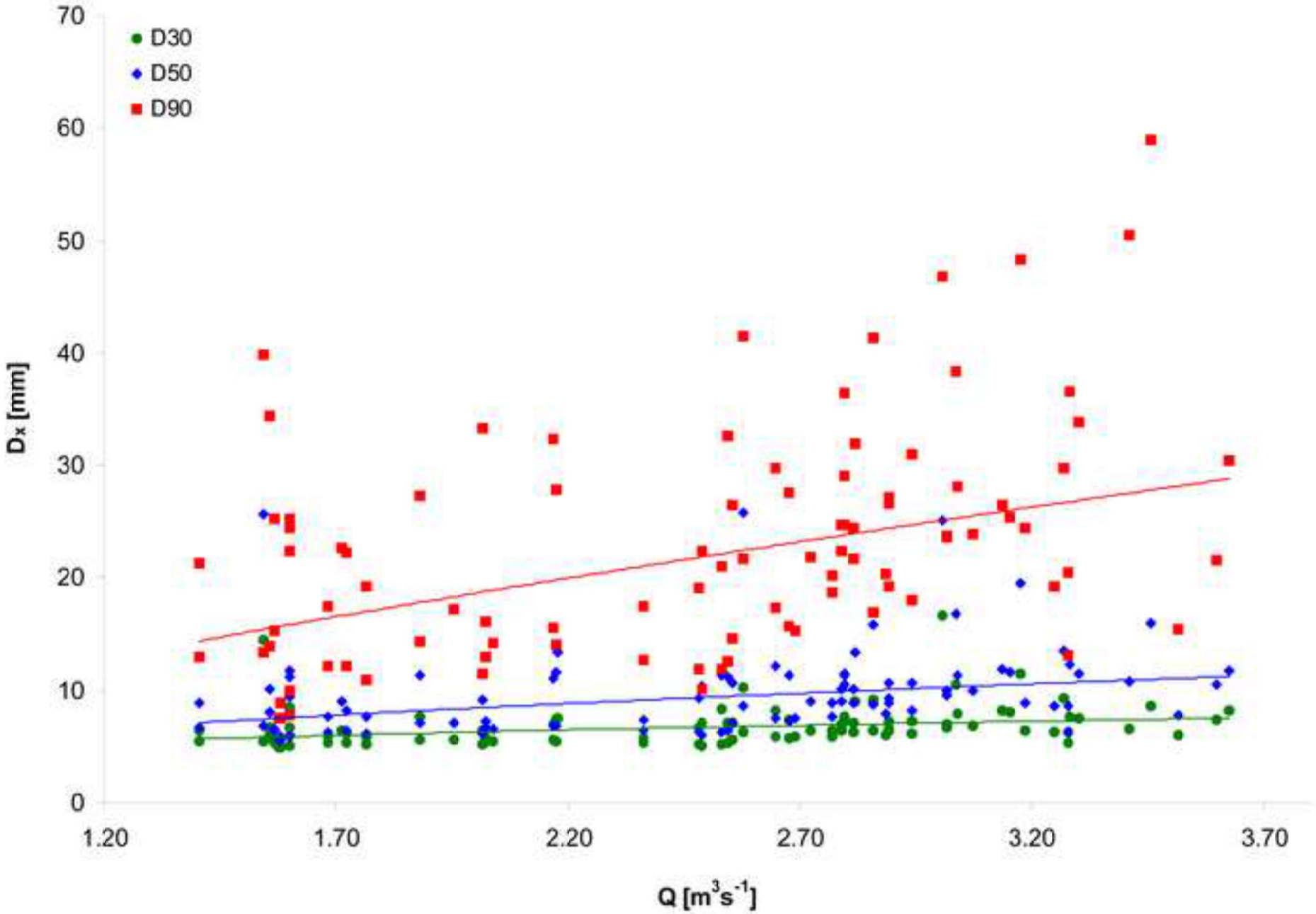

Figure 10

Click here to download high resolution image

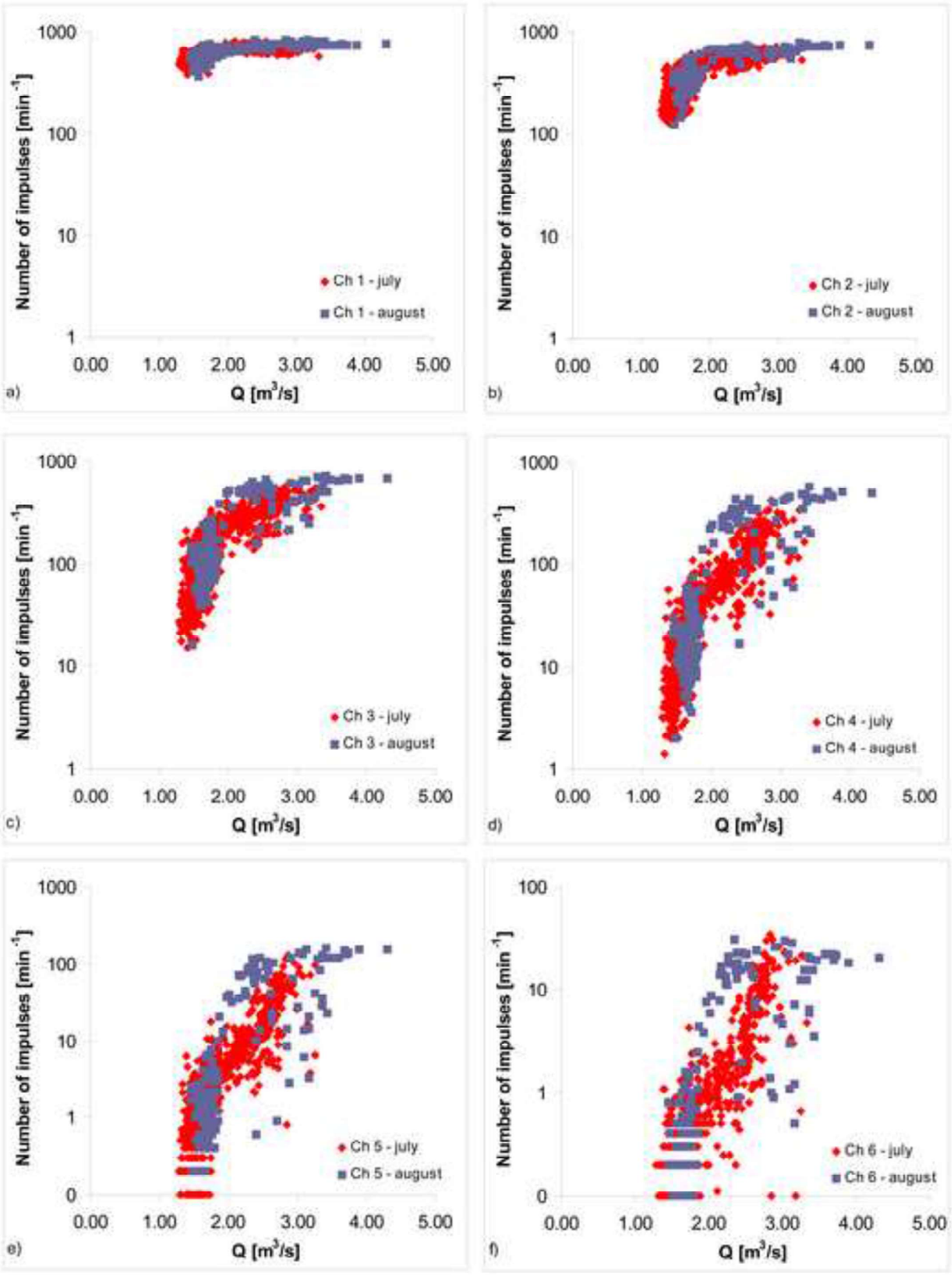

Figure 11
Click here to download high resolution image

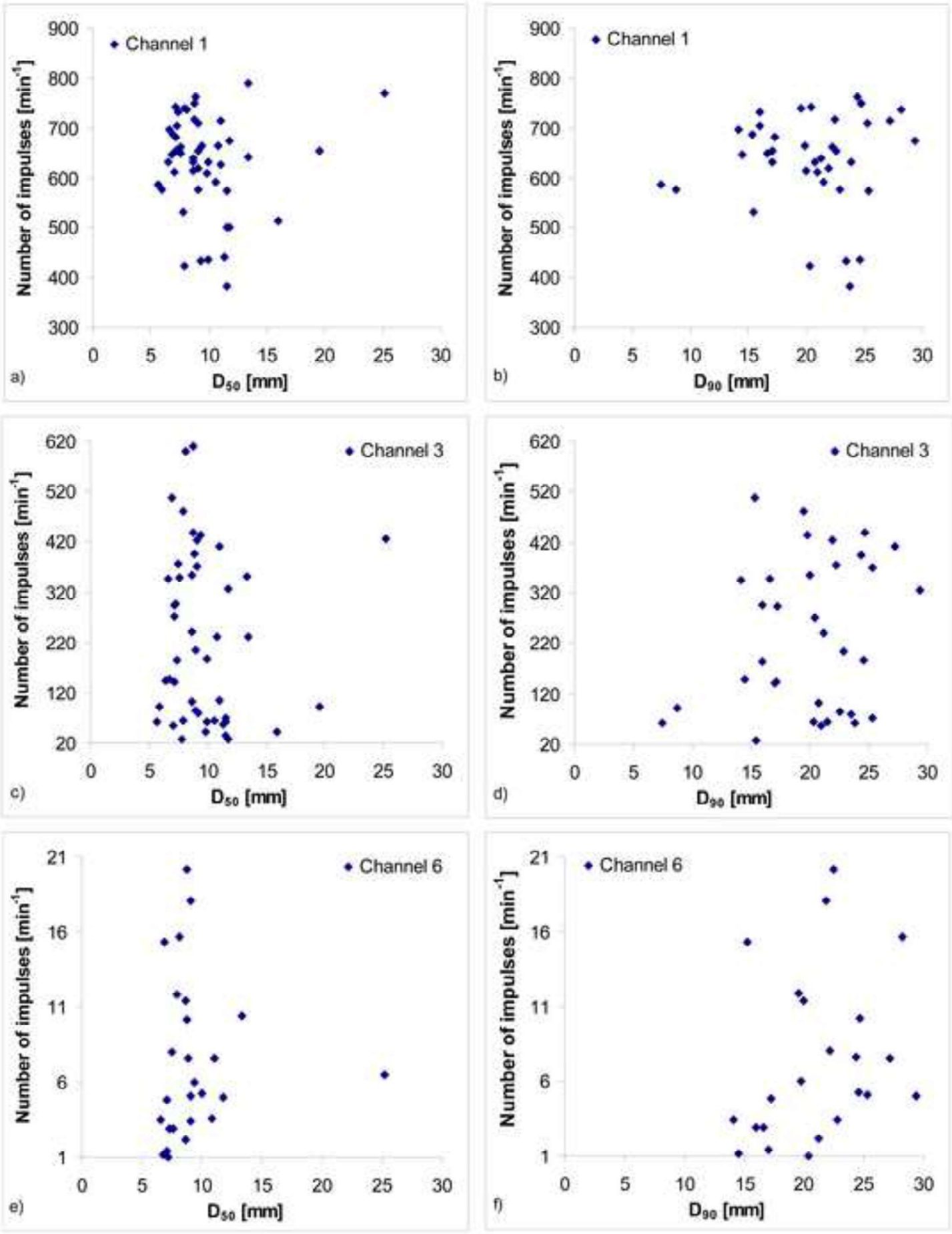

Figure 12
Click here to download high resolution image

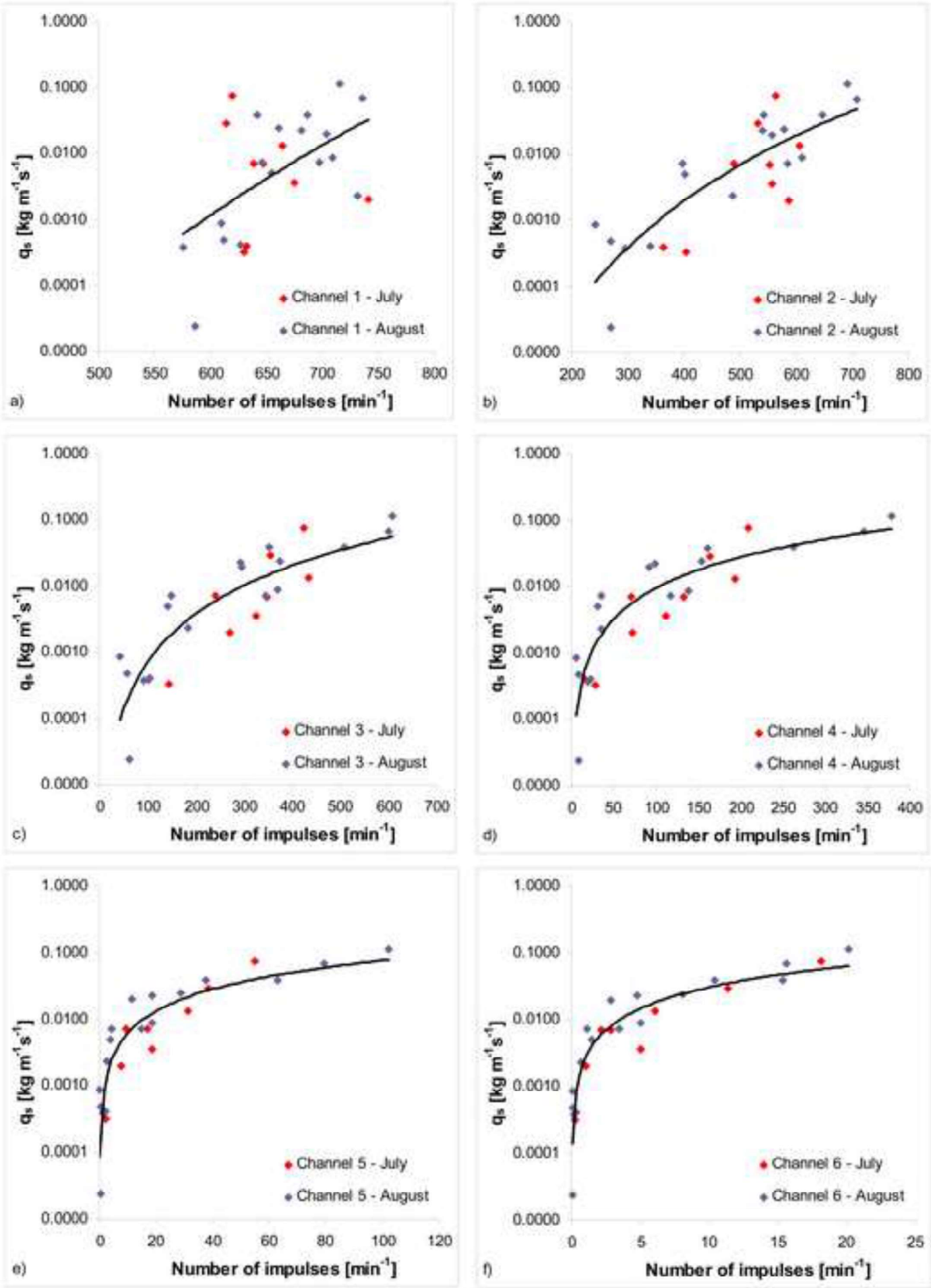

Table
Click here to download Table: Catena 2990 - Tables.doc

Table 1

Site	N	t [min]	Q [$m^3 s^{-1}$]	h [m]	q_s [kg $s^{-1} m^{-1}$]	w [kg]
A	55	6 – 63	1.4 – 3.6	0.22 - 0.37	$5.6*10^{-5}$ – $1.9*10^{-1}$	0.03 – 23.90
B	36	5 – 63	1.4 – 3.6	0.20 – 0.46	$1.6*10^{-4}$ – $1.9*10^{-1}$	0.18 – 14.85
C	4	15 - 30	1.6 – 2.0	0.43 – 0.46	$2.0*10^{-5}$ – $7.2*10^{-3}$	0.01 – 1.95

Table 2

Channel	Power law model						
	α	β	R^2	S_E (α)	S_E (β)	p (α)	p (β)
1	8.71E-20	6.14	0.09	0.0000	4.3061	>0.10	>0.10
2	3.93E-21	6.79	0.59	0.0000	1.4502	>0.10	>0.10
3	1.15E-09	2.84	0.76	0.0000	0.4459	<0.001	<0.001
4	5.51E-06	1.65	0.82	0.0000	0.2168	<0.001	<0.001
5	3.15E-04	1.26	0.91	0.0002	0.1222	<0.001	<0.001
6	5.31E-04	1.74	0.92	0.0003	0.1943	<0.001	<0.001

Channel	Linear model						
	A	B	R^2	S_E (A)	S_E (B)	p (A)	p (B)
1	-1.05E-01	1.89E-04	0.09	0.0786	0.0001	>0.10	>0.10
2	-4.50E-02	1.30E-04	0.38	0.0171	0.0000	<0.05	<0.001
3	-1.83E-02	1.34E-04	0.61	0.0071	0.0000	<0.05	<0.001
4	-8.01E-03	2.41E-04	0.77	0.0040	0.0000	<0.05	<0.001
5	-2.70E-03	9.93E-04	0.89	0.0024	0.0001	>0.10	<0.001
6	-3.36E-03	4.26E-03	0.87	0.0027	0.0003	>0.10	<0.001

Table 3

Channel	D30 [mm]	D50 [mm]	D84 [mm]	D90 [mm]	D100 [mm]
1	4.9	5.7	7.2	7.5	8.0
2	4.9	5.7	7.2	7.5	8.0
3	4.9	5.7	7.2	7.5	8.0
4	4.9	5.7	7.2	7.5	8.0
5	5.1	5.9	7.7	8.7	16.0
6	5.4	6.6	12.0	14.1	32.0